Korean J. Chem. Eng., 37(6), 1097-1106 (2020)
DOI: 10.1007/s11814-020-0532-3

pISSN: 0256-1115
eISSN: 1975-7220

A facile method to synthesize magnetic nanoparticles chelated with Copper(II) for selective adsorption of bovine hemoglobin

Huiyuan Guan, Jundong Wang, Siyuan Tan, Qiang Han, Qionglin Liang†, and Mingyu Ding†

MOE Key Laboratory of Bioorganic Phosphorus Chemistry and Chemical Biology, Ministry of Education, Department of Chemistry, Tsinghua University, Beijing 100084, China
(*Received 5 December 2019 • accepted 5 March 2020*)

Abstract−A novel and uncomplicated synthesis method of Cu^{2+}-chelating with carboxyl groups that directly-modified $NiFe_2O_4$ magnetic microspheres ($NiFe_2O_4$-PAA-Cu^{2+}) was fabricated for selective enrichment and separation of bovine hemoglobin (BHb). First, a carboxyl group directly-modified on $NiFe_2O_4$ magnetic microspheres was gained through a facile one-pot solvothermal method. Second, Cu^{2+} from $CuSO_4$ was brought into use to react with carboxyl groups under mechanical stirring at room temperature. The resulting magnetic microspheres were characterized by distinct instruments that included transmission electron microscopy (TEM), Brunauer-Emmett-Teller (BET), Fourier transform infrared spectroscopy (FT-IR), X-ray photoelectron spectroscopy (XPS), vibrating sample magnetometer (VSM) and scanning electron microscope (SEM) to examine the size, morphology, composition and magnetization characterization. The results indicated that the $NiFe_2O_4$-PAA-Cu^{2+} microspheres exhibited good saturation magnetization (36.686 emu g^{-1}), which can facilitate magnetic separation under the help of an outside magnetic field. Also, good dispersion and high adsorption ability to BHb (783.53 mg g^{-1}) can be applied to selective enrichment for bovine hemoglobin and used for selective sorption of BHb protein in bovine blood samples.

Keywords: Immobilized Metal Affinity Chromatography, Facile Synthesis, Magnetic Nanoparticles, Selective Separation, Bovine Hemoglobin

INTRODUCTION

Proteomics study has been gaining much attention due to its importance for tissues and organs of the human body; it also offers approaches for deeper understanding of the cellular metabolism process and the mechanisms of diseases [1-3]. Hemoglobin (Hb), as one of the abundant proteins that exist in red blood cells, is a histidine-rich protein [4]. It mainly functions as the carrier of oxygen, transports carbon dioxide as well as adjusts the acid-based balance of blood [5]; it plays an important role in the vascular system of the vertebrate. In addition, the level of hemoglobin is also considered as an indicator of many diseases, for example, heart diseases, anemia and some hereditary diseases [6-8]. However, there are some disadvantages caused by the high abundant hemoglobin. For example, the analysis of low abundant proteins was always interrupted by the highly abundant hemoglobin in the biological analysis, which would be an influence for detecting some components in blood [9]. Therefore, studying novel strategies of selective separation and removal of Hb is a critical step for proteomics studies and biomedical diagnosis. Compared with Hb, bovine hemoglobin (BHb) owns 90% amino acid sequence homology [10]; it also has a better ability in carrying oxygen and there are more histidine residues expose on the surface of BHb. Thus, BHb can be always used instead of Hb in histidine-rich protein preliminary studies to get a more obvious result [11,12].

To develop efficient and facile ways to get high capacity and purity of Hb for study and application, scientists paid hard effort in developing novel methods in selective separation of Hb or BHb from complicated biomarkers [13]. The various reported protocols include immobilized metal affinity chromatography (IMAC) [14-17], metal oxide affinity chromatography (MOAC) [18-20] and molecular imprinting technique (MIT) [21-23]. IMAC is one of the most general methods for selective enrichment of proteins, especially for his-rich proteins. Yang et al. synthesized a sandwich-like structure graphene oxide coated with polydopamine-Ni^{2+} for carrying out high performance in histidine-rich BHb separation [24]. Zhang et al. developed an iminodiacetic acid (IDA)-base magnetic nanoparticles that chelated with Cu^{2+} and Fe_3O_4/dopamine/Au nanocomposites that functionalized by IDA chelated with Cu^{2+} for highly selective BHb separation and depletion [25,26]. Zhang et al. reported the poly(vinyl alcohol-co-ethylene) nanofibrous membrane was functioned with Ni^{2+}-chelated ligand for BHb adsorption [27]. However, there were some disadvantages reflected in their particle application during protein isolation. First, IDA and nitrilotriacetic acid (NTA) are two of the most general chelating linkers. However, this method needs tedious steps and plenty of time to bind the linker to the substrate [28]. Furthermore, due to the weak chelation between metal ions and linkers, the chelated metal ions could be easily gone during the experimental process [29,30]. Second, to synthesize the polymer membrane needed for complex experimental conditions, such as oxygen-free, complex experimental instruments and low-temperature operation. Although spending much time and

†To whom correspondence should be addressed.
E-mail: liangql@mail.tsinghua.edu.cn, dingmy@mail.tsinghua.edu.cn
Copyright by The Korean Institute of Chemical Engineers.

using a complex method to synthesize the adsorbent, the nonspecific adsorption of other proteins and the unsatisfactory adsorption capacity of BHb were unavoidable. To correct these problems, it is urgent to develop novel and efficient approaches in selective adsorption histidine-rich proteins from the complex biological samples.

Nanomaterial owns different properties from the macroscopic substance, including small size effect, high surface effect, and quantum size effect [31-33]. Among the nanomaterials, magnetic nanoparticles (MNPs) possess a superparamagnetic property which ordinary nanomaterial does not. Under the external magnetic field, magnetic nanoparticles can be quickly and effortlessly separated from the sample solution, leading to high separating efficiency and environmental-friendly results. Magnetic nanoparticles can be further functionally grafted through directly doping with other metal ions and modified with the functional groups to be convenient for the following needs [34-38]. Thus, the study and application of magnetic nanoparticles and magnetic nanocomposites have drawn the attention of scientists because magnetic materials are widely applied in bio-imaging, drug storage and delivery as well as separation science and catalysis [39,40]. In recent years, in order to make up the shortcoming in IMAC, IMAC combined with magnetic nanomaterial was developed and applied in separation science [41-45].

In this work, we have successfully proposed a novel and facile approach for the fabrication of poly(acrylic acid) (PAA) modified magnetic $NiFe_2O_4$ nanoparticles carrying immobilized Cu^{2+} (marked as $NiFe_2O_4$-PAA-Cu^{2+}) for selective adsorption of bovine hemoglobin. The resultant material showed favorable adsorption capacity and fast adsorption time of bovine hemoglobin. The prepared magnetic nanoparticles were characterized by several characterization equipment, for example, TEM, SEM, FT-IR, XPS, VSM, and BET. To examine the most suitable adsorption capability, the magnetic nanoparticles and adsorption conditions were investigated and optimized. Furthermore, they also successfully exhibited notable application in selective adsorption and enrichment of bovine hemoglobin from real biological sample of bovine blood.

EXPERIMENTAL SECTION

1. Chemicals and Materials

Ethylene glycol (EG) and diethylene glycol (DEG) were received from Sinopharm Chemical Reagent Beijing Co., Ltd. Nickel(II) chloride anhydrous ($NiCl_2$) was brought from Beijing InnoChem Science & Technology Co., Ltd. Iron chloride hexahydrate ($FeCl_3{\cdot}6H_2O$) was acquired from Xilong Chemical Co., Ltd (Guangdong, China). Cupric sulfate anhydrous ($CuSO_4$) was bought from Shanghai Macklin Biochemical Co., Ltd (Shanghai, China). Poly(acrylic acid) (PAA) was supplied by Keao Biotech Co., Ltd. (Beijing, China). Tris(hydroxymethyl) aminomethane (Tris) was purchased from J&K Chemicals (Beijing, China). Sodium hydroxide (NaOH), Sodium citrate, Sodium acetate (C_2H_5ONa) and hydrochloric acid (HCl) were acquired from Beijing Chemical Works (Beijing, China). Sodium dodecyl sulfate (SDS) was bought from Tianjin Fuchen chemical reagents factory (Tianjin, China). All above chemical reagents listed were all analytical reagent grade and were employed directly without any other purification or modification, deionized water was used throughout this work.

Proteins including bovine serum albumin (BSA, MW 67 kDa, pI 4.7), bovine hemoglobin (BHb, MW 64.5 kDa, pI 6.8), Cytochrome C (Cyt-c, MW 12.4 kDa, pI 10.2), Lysozyme (Lyz, MW 14 kDa, pI 11.2), Ovalbumin (OVA, MW 44.5 kDa pI 4.7), Horseradish peroxidase (HRP, MW 40 kDa, pI 7.2) and bovine plasma were all purchased from Beijing Keao Biological Pharmaceutical Co., Ltd (Beijing, China). β-Lactoglobulin (β-Lac, MW 18 kDa, pI 5.2) was purchased from Sigma-Aldrich (St. Louis, MO, USA).

2. Characterization

U-3900 UV-vis spectrophotometer (Hitachi, Japan) was used to evaluate the adsorption capacity of proteins. A type of H-7650B (Hitachi, Japan) was used for obtaining the transmission electron microscopy (TEM) images. The magnetization curves of resultants were assessed by a vibrating sample magnetometer (VSM) (Quantum Design, USA). X-ray photoelectron spectroscopy (XPS) was performed on a Thermo Scientific Escalab 250Xi spectrometer (UK). Fourier transform infrared (FT-IR) spectra in KBr were noted on a Bruker Fourier transform infrared spectrometer (Horiba, Germany) within a range from 4,000 to 400 cm^{-1}. Morphological structures were given out by an SU-8010 field emission scanning electron microscope (SEM, Hitachi, Japan). The Brunauer-Emmett-Teller (BET) specific surface area results were carried out from an ASAP 2010C analyzer (Micromeritics, USA). A Delta 320 pH Meter (Mettler Toledo, China) was used for measuring the pH of buffers.

All chromatographic results were from an Agilent 1100 series high performance liquid chromatography (HPLC) system (Agilent, USA) and an Agilent ZORBAX 300SB-C18 (250 mm×4.6 mm, 5 μm, 300 °A) column (Agilent, USA). The proteins were eluted by buffer B with a linear gradient from 5% to 75% (buffer A, 0.1% TFA in water; buffer B, ACN) over 45 min with the flow rate of 1.0 mL min^{-1}. Every injected sample volume was 25 μL, and the samples were detected using a UV detector (215 nm for BSA, BHb and Lyz).

An assay of sodium dodecyl sulfate polyacrylamide gel electrophoresis (SDS-PAGE), which was from Beijing Liuyi Biotechnology Co., Ltd, China, with 15% running and 5% stacking, was used to gain the electrophoresis of proteins. Proteins were stained with Coomassie Brilliant Blue R-250.

3. Synthesis of $NiFe_2O_4$-PAA-Cu^{2+} Microspheres

3-1. Preparation of $NiFe_2O_4$-PAA Nanoparticles

The whole schematic procedure for the magnetic $NiFe_2O_4$-PAA-Cu^{2+} microspheres is illustrated in Fig. 1. First, the $NiFe_2O_4$-PAA magnetic nanoparticles were synthesized by a solvothermal reaction at 200 °C. Briefly, $FeCl_3{\cdot}6H_2O$ (1.08 g, 4.0 mmol), $NiCl_2$ (0.26 g, 2.0 mmol), sodium acetate (4 g) and PAA (0.1 g) were dissolved in the mixture of DEG (26 mL) and ethylene glycol (14 mL) under stirring until solids dissolved completely. Subsequently, the resultant became a homogeneous deep green solution, and then transferred into a Teflon-lined stainless-steel autoclave (capacity of 100 mL), sealed and reacted at 200 °C for 10 h. After reaction, the autoclave was chilled to room temperature. The obtained deep brown magnetic particles were rinsed with water three times. Eventually, the obtained product was collected by a magnet and dried in freeze-drying vacuum for 24 h.

3-2. Preparation of $NiFe_2O_4$-PAA-Cu^{2+} Microspheres

The $NiFe_2O_4$-PAA-Cu^{2+} nanospheres were prepared by a simple one-step method. Dried $NiFe_2O_4$-PAA (0.1 g) magnetic nanoparti-

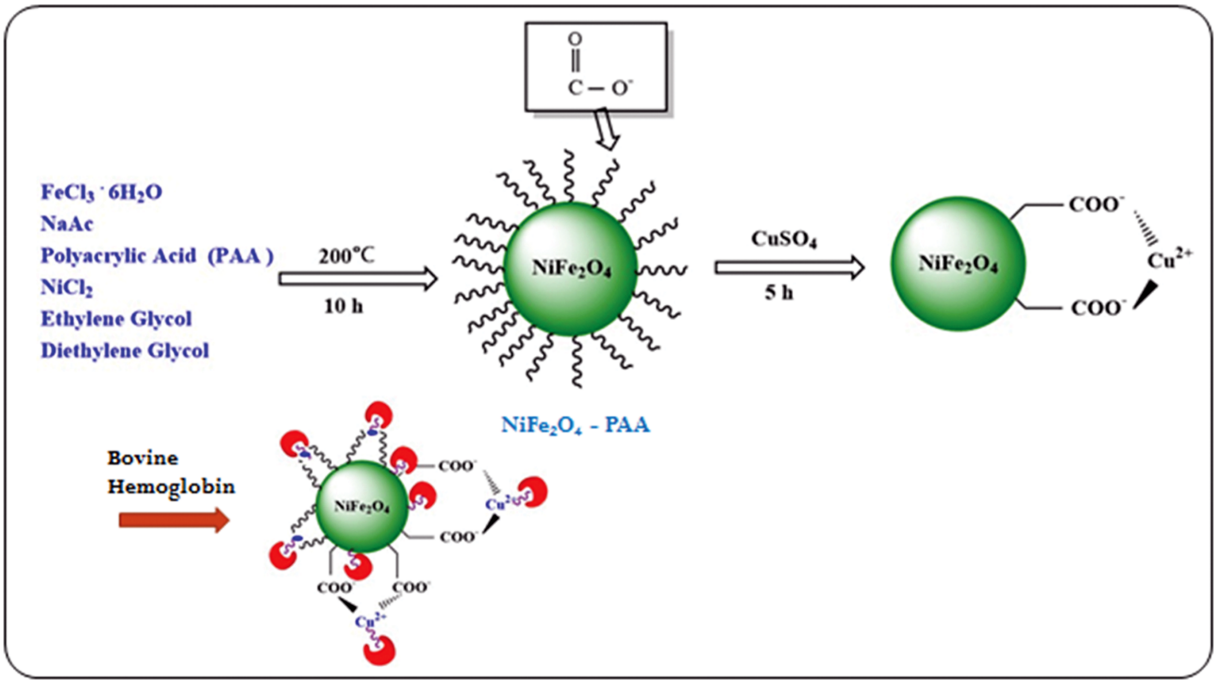


Fig. 1. Schematic diagram of the synthesis movement for the $NiFe_2O_4$-PAA-Cu^{2+} magnetic microspheres.

cles were well dispersed in 100 mL of 2.5 g $CuSO_4$ solution. The reaction mixture was reacted at room temperature for 5 h under mechanical stirring. The obtained deep brown magnetic particles were rinsed three times with water. Finally, the obtained product was obtained by a magnet and then dried in freeze-drying vacuum for 24 h.

4. Selectivity Experiments

The non-bovine hemoglobin proteins (including BSA, Cyt-c, Lyz, HRP, OVA and β-Lac) and a mixture sample of various proteins (including BSA, Lyz and BHb) were dissolved in Tris-HCl buffer (pH=7.0). To each 1 mL above protein solution was added 1 mg of magnetic particles, and then incubated at room temperature for three hours; the captured species were eluted with 1 mL of 0.5%wt SDS for 1.5 h. Finally, the initial solutions, the supernatant solutions and the eluted solutions were measured by UV-Vis spectrophotometer with wavelength of 406 nm or HPLC.

5. BHb Adsorption Experiments

In this part, in order to study the influence of changing conditions on the resulting microspheres, BHb had been the aimed protein to conduct analysis. We discussed the adsorption capacity of BHb to the $NiFe_2O_4$-PAA-Cu^{2+} microspheres in different influences of changing initial BHb concentration, pH of environment, adsorption time and ionic strength. The whole relative BHb adsorption experiments were all gone through with a 2 mL of centrifugal tube. Generally, 1 mg of $NiFe_2O_4$-PAA-Cu^{2+} microspheres was dispersed in 1 mL of BHb solution (dissolved in Tris-HCl as buffer) and then incubated at room temperature for three hours. When adsorption was done, the microspheres were gathered by an outside magnet; there was some remaining BHb in the supernatant that was not adsorbed by the resultant microspheres; this part of BHb was investigated by UV-Vis spectrophotometer.

6. Select of Eluting Reagents and Reusability of Prepared $NiFe_2O_4$-PAA-Cu^{2+} Microspheres

The reusability of $NiFe_2O_4$-PAA-Cu^{2+} microspheres was investigated next. Various eluting reagents were used to test the ability for recovery of the adsorbed BHb as follows: 1 mg of $NiFe_2O_4$-PAA-Cu^{2+} microspheres was dispersed in 1 mL of 0.8 mg mL^{-1} BHb solution and incubated in room temperature 3 h. After magnetic collecting of the microspheres, the adsorbent was washed by the Tris-HCl buffer (pH=7.0) for three times. After that, 1 mL of 0.5%wt SDS, 0.5%wt Histidine, 0.1 M of Tris-HCl (pH=9.0), NaOH and sodium citrate were used to recover the adsorbed BHb, respectively, and then shaken at room temperature for 1.5 h. After the solid products were aggregated under the attraction of an external magnet, the recovered BHb in supernatant was detected by using UV-Vis spectrophotometer, the microspheres and then rinsed with Tris-HCl buffer (pH=7.0) and water for several times, then continued with the same steps for next adsorption-desorption cycle of BHb.

7. Real Biological Sample Experiment

In this part, bovine plasma was as real biological sample to test the last performance of $NiFe_2O_4$-PAA-Cu^{2+}. Tris-HCl (pH=7.0) with 0.1 mg mL^{-1} of BHb was added to bovine plasma to make a 20-fold diluted solution (marked as BP-1) as a sample of pre-real sample analysis and following the sorption process as mentioned above. After the separation with an external magnet, the supernatant was measured through the UV-Vis spectrophotometer.

Tris-HCl (pH=7.0) with 0.2 mg mL^{-1} of BHb was added to bovine plasma to make a 20-fold diluted solution (marked as BP-2) and was incubated with $NiFe_2O_4$-PAA-Cu^{2+} microspheres. Then the BHb-adsorbed microspheres were eluted with 1 mL of 0.5%wt SDS solution. For the initial solution, the supernatant solution and the eluted solution and a 0.2 mg mL^{-1} of BHb (pH=7.0 Tris-HCl as buf-

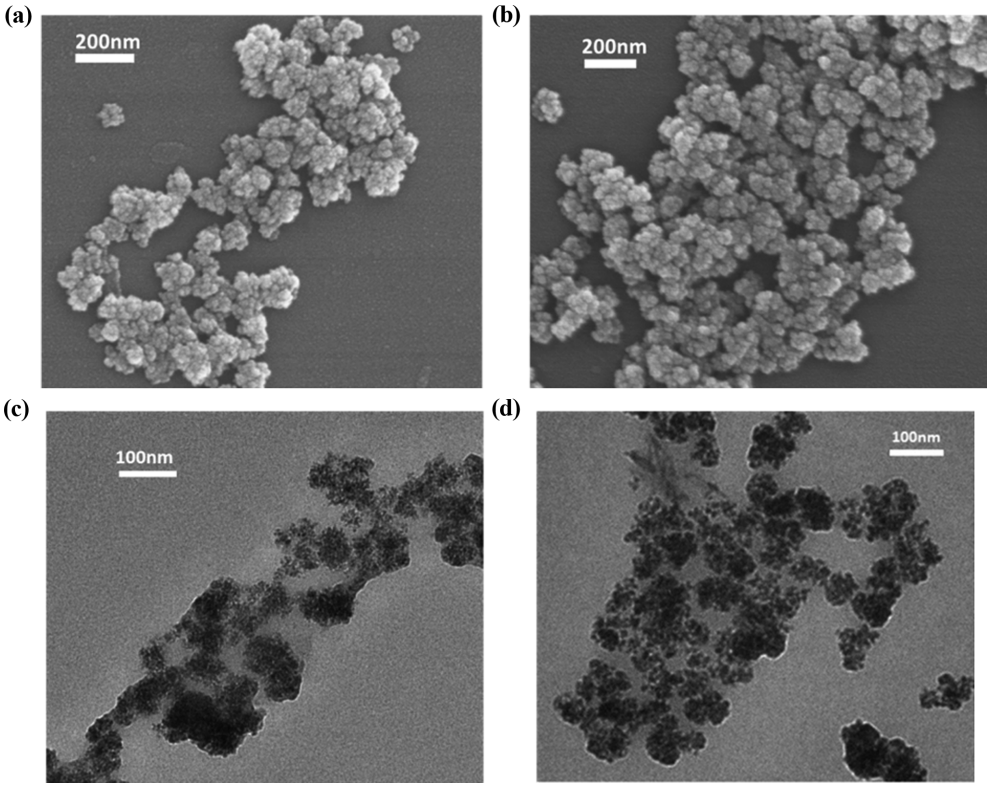


Fig. 2. SEM results of $NiFe_2O_4$-PAA (a) and $NiFe_2O_4$-PAA-Cu^{2+} (b). TEM results of $NiFe_2O_4$-PAA (c) and $NiFe_2O_4$-PAA-Cu^{2+} (d).

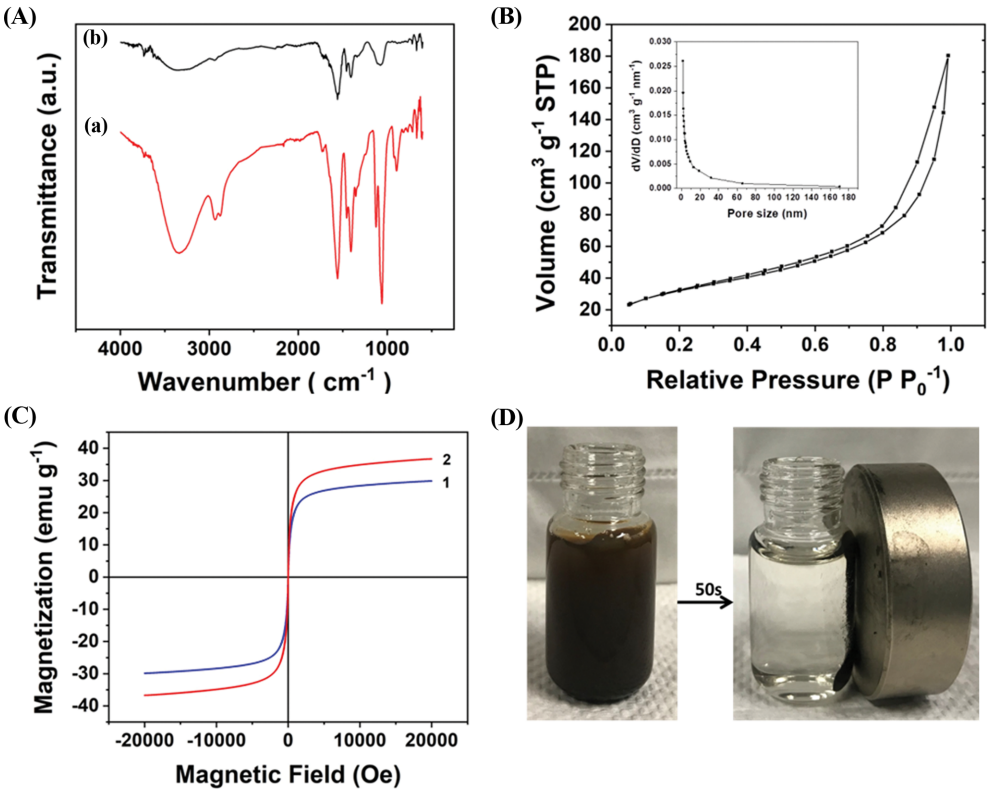


Fig. 3. (A) FT-IR spectra of the $NiFe_2O_4$-PAA (a) and $NiFe_2O_4$-PAA-Cu^{2+} (b) microspheres. (B) N_2 adsorption/desorption isotherms, pore size distribution curve of $NiFe_2O_4$-PAA-Cu^{2+} microspheres. (C) Magnetization curves of the $NiFe_2O_4$-PAA (1) and $NiFe_2O_4$-PAA-Cu^{2+} (2) microspheres. (D) The dispersion and separation process of $NiFe_2O_4$-PAA-Cu^{2+} microspheres.

fer), every sample amount was 20 μL, using SDS-PAGE to analyze.

RESULTS AND DISCUSSION

1. Characterization Results of $NiFe_2O_4$-PAA and $NiFe_2O_4$-PAA-Cu^{2+} Microspheres.

The morphology of obtained microspheres was further studied by using TEM in order to refer the particles having spherical-like morphology and uniform sizes. In Fig. 2(c) and Fig. 2(d), the TEM images of the $NiFe_2O_4$-PAA and $NiFe_2O_4$-PAA-Cu^{2+} microspheres are shown, respectively; it can be seen that the sizes of $NiFe_2O_4$-PAA average diameter range from 6 nm to 10 nm and exhibit agglomeration resulting from drying process; no significant size change could be observed after chelating with Cu^{2+} ions, but the sphericity of $NiFe_2O_4$-PAA-Cu^{2+} microspheres was more obvious and clear. Although also exhibiting agglomeration resulting from the drying process, every $NiFe_2O_4$-PAA-Cu^{2+} microsphere showed a clearer shape and the SEM images (Fig. 2(a) and Fig. 2(b)) gave the same result.

The FT-IR spectra of $NiFe_2O_4$-PAA and $NiFe_2O_4$-PAA-Cu^{2+} are exhibited in Fig. 3(A). Both of two FT-IR spectra show adsorption peaks around 3,363 cm^{-1} and adsorption shape peaks around 1,058 cm^{-1}, which were the characteristic bands of stretching vibration and bending vibration of hydroxyl functional group (O-H) on the $NiFe_2O_4$-PAA and $NiFe_2O_4$-PAA-Cu^{2+} surface, respectively [46,47]; the peaks at 2,931 cm^{-1} and 2,873 cm^{-1} are the -CH_2 bond from poly(acrylic acid) (PAA [48]. Besides, the peaks at 1,558 cm^{-1} and 1,406 cm^{-1} were ascribed to the symmetric stretching vibration and asymmetric stretching vibration of carboxylate groups, respectively. This consequence showed that carboxyl groups were modified on the surface of $NiFe_2O_4$-PAA well. Furthermore, it was obvious that after chelating with Cu^{2+}, the intensity of stretching vibration and bending vibration of hydroxyl functional group (O-H) and the stretching vibrations of symmetric COO^-, asymmetric COO^- were weaker than before, which illustrated that carboxylate groups were chelated with Cu^{2+} ions, so consuming the carboxylate groups and making the intensity of carboxylate groups decreased. As we could notice in the FT-IR spectra, there were two low wavenumber peaks referred to the spinel structure of $NiFe_2O_4$; the peaks located at 667 cm^{-1} and 607 cm^{-1} refer to Ni-O and Fe-O stretching vibrations [49]. To conclude this part, it is reasonable that $NiFe_2O_4$-PAA and $NiFe_2O_4$-PAA-Cu^{2+} were obtained successfully.

To illustrate Cu^{2+} ions were chelated with $NiFe_2O_4$-PAA in the second step of synthesis process, XPS examination result shows the extra review of the chemical composition of $NiFe_2O_4$-PAA and $NiFe_2O_4$-PAA-Cu^{2+} microspheres. As shown in XPS spectra Fig. S1(a), $NiFe_2O_4$-PAA contained elements including C, O, Fe, Ni, Na; the element Na might come from the completely unreacted sodium acetate. As shown in XPS spectra Fig. S1(b), $NiFe_2O_4$-PAA-Cu^{2+} contained elements including, C, O, Fe, Ni, Cu; this result indicated that after binding with Cu^{2+} in the second step, Cu^{2+} ions were successfully chelated with $NiFe_2O_4$-PAA and the residual Na^+ ions were cleared through the second step reaction.

The BET results showed the surface areas were 53.066 m^2 g^{-1} and 119.12 m^2 g^{-1}; the total pore volumes were 0.35 cm^3 g^{-1} and 0.277 cm^3 g^{-1} for $NiFe_2O_4$-PAA and $NiFe_2O_4$-PAA-Cu^{2+} microspheres, respectively. The surface area was increased a double after introducing of Cu^{2+} ions, magnetic microspheres were charged with the same charge and repulsed each other. The N_2 adsorption-desorption isotherms and the pore size distribution curve for $NiFe_2O_4$-PAA and $NiFe_2O_4$-PAA-Cu^{2+} microspheres are shown in Fig. S3 and Fig. 3(B). $NiFe_2O_4$-PAA and $NiFe_2O_4$-PAA-Cu^{2+} microsphere results both illustrated that there are irregular mesopores which existed in two prepared-microspheres. The images exhibit Type II isotherm with a small Type H3 hysteresis, caused by the space among the accumulated particles; little twisted mesopore channels and the heterogeneity in the adsorbent-adsorbed substance interactions [50-53].

The saturation magnetization (Ms) is a key property and determining factor of magnetic materials; thus VSM was used for investigating the magnetism of $NiFe_2O_4$-PAA and $NiFe_2O_4$-PAA-Cu^{2+} microspheres at room temperature, and the results are shown at Fig. 3(C). The Ms values of $NiFe_2O_4$-PAA and $NiFe_2O_4$-PAA-Cu^{2+} microspheres are 29.85 emu g^{-1} and 36.68 emu g^{-1}, respectively. After chelating with Cu^{2+} ions to the carboxylate groups on the surface of $NiFe_2O_4$-PAA (curve 2), the saturation magnetization value was increased from 29.85 emu g^{-1} to 36.68 emu g^{-1}; it can be attributed to the introducing of Cu^{2+} ions [54]. With the increasing of saturation magnetization value, it means the resultant particles have superparamagnetic properties, and it is enough for using in magnetic separation. Moreover, Fig. 3(D) shows the dispersion and separation process of $NiFe_2O_4$-PAA-Cu^{2+} microspheres. $NiFe_2O_4$-PAA-Cu^{2+} microspheres display a good dispersion in water. When the magnet approached to the mixture, the resultant magnetic material could be rapidly separated by a magnet within 50 seconds. Thus, the result confirmed that the great magnetism of $NiFe_2O_4$-PAA-Cu^{2+} microspheres can be used for separation of proteins and reduce traditional complex separation steps and be time-saving.

2. The Influence of pH and Ionic Strength

For the propose of exploring the impact of different pH on adsorption behavior, a single component of proteins was applied to conduct a series of adsorption experiments, which included BHb, OVA and β-Lac, at different pH studied. Fig. 4(a) illustrates the adsorption behavior of BHb, OVA and β-lac on $NiFe_2O_4$-PAA-Cu^{2+} microspheres in different pH values, and the result has improved the adsorption capacity of protein much depended on pH value. As Fig. 4 shows, when pH=7.0, the microspheres could reach the maximum adsorption quantities to BHb and this pH value is much close to the pI of BHb. The pH value whether being up or down, the adsorption capacity of BHb was significantly reduced. The other two proteins OVA and β-Lac reached maximum adsorption capacity when pH at 4.0 and 6.0, respectively, which is quite near to their pI (±0.8). When the pH was getting closer to the pI of proteins, it would lead the inner hydrophobic residues of proteins to be exposed easily. Other than this, there is the same phenomenon when the pH value was raised or reduced from pI; the adsorption capacity of OVA or β-Lac got a significant decrease too. Commonly, proteins with suitable electron-donor groups can coordinate with metal ions on the surface of IMAC material. BHb is a kind of protein that is rich in histidine residues; there are 24 histidine residues exposed on the surface of BHb [55]. Under the condition of neutral pH value, histidine of BHb is the main amino acid that

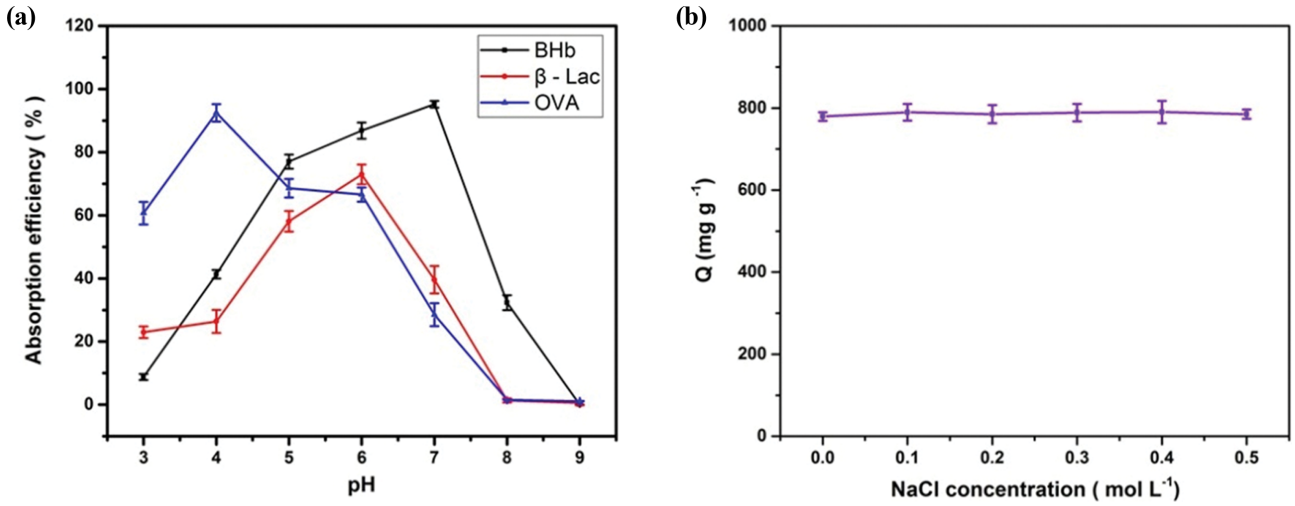


Fig. 4. (a) Effects of pH on adsorption properties of the $NiFe_2O_4$-PAA-Cu^{2+} microspheres. (b) The effect on ionic strength to the changing adsorption ability to BHb of $NiFe_2O_4$-PAA-Cu^{2+} microspheres.

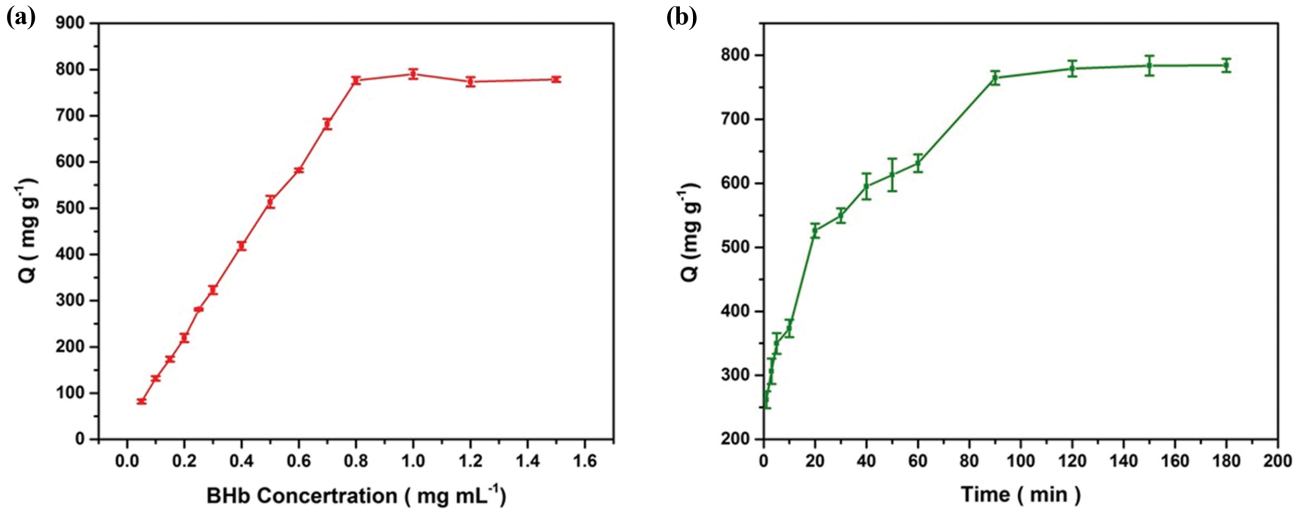


Fig. 5. Adsorption isotherms (a) and adsorption kinetics (b) of BHb on $NiFe_2O_4$-PAA-Cu^{2+} microspheres.

binds to the metal ions, so it performs a maximum adsorption capacity when pH=7.0; under these optimum conditions, the adsorption efficiency of BHb is higher than those of OVA and β-Lac. Therefore, pH=7.0 was chosen as a condition of the follow-up experiments. In addition, with the existence of certain concentration of NaCl, the effect on ionic strength to the changing adsorption ability of BHb of $NiFe_2O_4$-PAA-Cu^{2+} was studied. Obviously, Fig. 4(b) shows that there is almost no impact on adsorption of BHb with the ionic strength changed within a certain range; the concentration of NaCl in BHb was maintained at a concentration up to 0.5 mol/L. The result in Fig. 4(b) illustrates that $NiFe_2O_4$-PAA-Cu^{2+} microspheres are practical in treating real biological samples with relatively certain ionic strength.

3. The Influence of BHb Concentration and Adsorption Time

To assess the adsorption capacity of BHb on $NiFe_2O_4$-PAA-Cu^{2+} microspheres, an experiment was conducted at room temperature with the BHb concentration range 0.05-1.5 mg mL^{-1}. Fig. 5(a) illustrates the maximum adsorption capacity of resultant microspheres; the initial adsorption capacity of resultant microspheres increased along with the developing concentration of BHb. The adsorption equilibrium could be reached when the concentration of BHb was raised to 0.8 mg mL^{-1}; the adsorption ability of resultant microspheres got a little variation until the concentration reached 1.5 mg mL^{-1}. It shows the maximum experimental adsorption capacity of $NiFe_2O_4$-PAA-Cu^{2+} microspheres is determined to be 783.53 mg g^{-1} which got a greater adsorption capacity than various adsorbents (Table 1). The Langmuir model and Freundlich model were employed to evaluate the theoretical adsorption capacity of $NiFe_2O_4$-PAA-Cu^{2+} that is shown in Fig. S2(a) and (b); the result was that the experimental adsorption isotherms accorded closely to the Langmuir model, the maximum adsorption quantity 800 mg mL^{-1} which matched to the experimental adsorption capacity. In the condition of 0.8 mg mL^{-1} of BHb as initial concentration, the adsorption kinetics was studied at different adsorption time of range 0-180 min. As illustrated in Fig. 5(b), the resultant microspheres got more than half of the maximum adsorption capacity in 20 minutes,

Table 1. The contrast of adsorption capacity of BHb with a series of adsorbents

The comparing adsorbents	Adsorption capacity (mg g^{-1})	Reference
Cu^{2+}-mediated magnetic MIP	232.6	[56]
Magnetic DES-MIPs	169.32	[57]
Cu^{2+}-IDA-silica-coated magnetite sub-microspheres	418.6	[58]
Fe_3O_4@BHb-MIPs	37.58	[59]
Fe_3O_4-PEI-PA-Yb^{3+} MNPs	344.83	[60]
Cu^{2+}-IDA-poly(glycidyl methacrylate)-Fe_3O_4	135.7	[61]
$NiFe_2O_4$-PAA-Cu^{2+}	783.53	this work

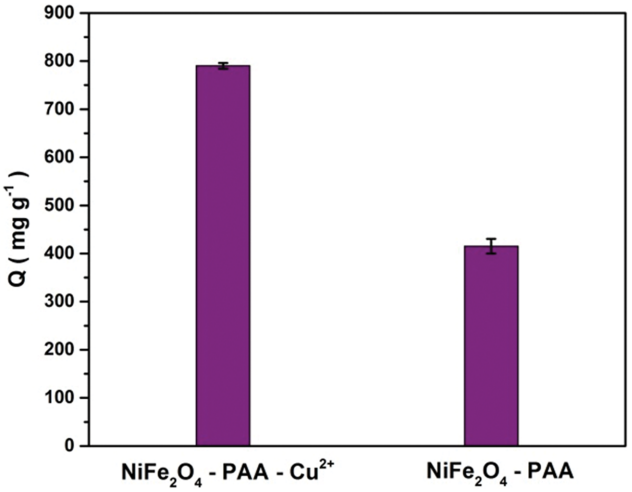


Fig. 6. Comparison with BHb adsorption on $NiFe_2O_4$-PAA and $NiFe_2O_4$-PAA-Cu^{2+} microspheres.

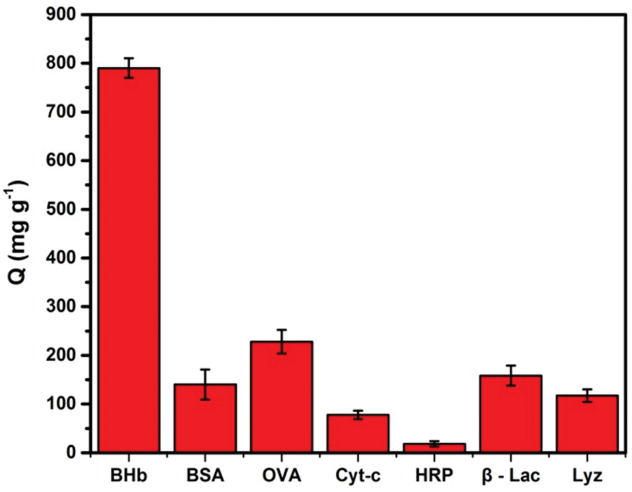


Fig. 7. Recognition of $NiFe_2O_4$-PAA-Cu^{2+} microspheres to different proteins.

the adsorption equilibrium and saturated adsorption reached within 180 min, achieved the maximum adsorption capacity about 98% at 120 min and reached adsorption equilibrium at 120 min. The result indicates that hemoglobin can be adsorbed by $NiFe_2O_4$-PAA-Cu^{2+} microspheres within a short time. The great adsorption ability might contribute by the affinity interaction among the metal ions, the histidine residues and carboxyl groups of BHb.

4. Comparison with $NiFe_2O_4$-PAA and $NiFe_2O_4$-PAA-Cu^{2+} Microspheres

$NiFe_2O_4$-PAA microspheres and $NiFe_2O_4$-PAA-Cu^{2+} microspheres are used to adsorb BHb under equal conditions in order to compare and interpret the superior of $NiFe_2O_4$-PAA-Cu^{2+} microspheres. As shown in the Fig. 6, compared with the $NiFe_2O_4$-PAA-Cu^{2+} microspheres, there was a small amount of adsorbed BHb discovered on the $NiFe_2O_4$-PAA microspheres. This phenomenon might be caused by the histidine residues of BHb being chelated with the carboxyl groups and NiO in the $NiFe_2O_4$-PAA microspheres or hydrophobic interaction. The predominant adsorption performance of $NiFe_2O_4$-PAA-Cu^{2+} microspheres might be mainly attributed by not only the histidine residues of BHb being chelated with the carboxyl groups and NiO, but also chelated with the Cu^{2+}, the Cu^{2+} as a co-functional monomer causing more binding sites in the surface of the $NiFe_2O_4$-PAA nanoparticles. This indicates that Cu^{2+} plays a critical part in BHb-adsorbed; the behavior from the histidine residues and carboxyl groups of BHb and NiO through coordination effect as assistance to enhance adsorption ability.

5. Selectivity of $NiFe_2O_4$-PAA-Cu^{2+} Microspheres for Proteins

In this part, BHb was compared with six other proteins that have different isoelectric points and molecular weights (including BSA, β-Lac, OVA, Cyt-c, HRP and Lyz) to prove the selectivity of $NiFe_2O_4$-PAA-Cu^{2+} microspheres to the target protein - BHb. As shown in Fig. 7, the $NiFe_2O_4$-PAA-Cu^{2+} microspheres presented a greater adsorption capacity for the target protein BHb than the other proteins under same conditions. However, it exhibits different binding capacity for every protein. It might be caused by the following reasons: for the BSA and Cyt-c, there are two histidine residues surface-exposed in BSA, while one histidine residue surface exposed on Cyt-c [62], so that the metal ions can chelate and be generated this adsorption. When pH=7.0, isoelectric points of the β-Lac and OVA were lower than environment pH, so the electrostatic interactions led to the adsorption for β-Lac and OVA; as to Lyz, isoelectric points of the Lyz were higher than environment pH, but some exposed histidine residues of Lyz could be chelated with Cu^{2+} to cause a minor adsorption [63]. On the other hand, HRP is a kind of glycoprotein, in which the protein size is much larger than the size of pore size even the resultant microspheres, resulting in the size-exclusion effect caused by the small amount of adsorption capacity for HRP. Furthermore, a stricter test for the selectivity of $NiFe_2O_4$-PAA-Cu^{2+} microspheres for BHb was tested by HPLC in which protein mixed solution which included Lyz, BSA and BHb

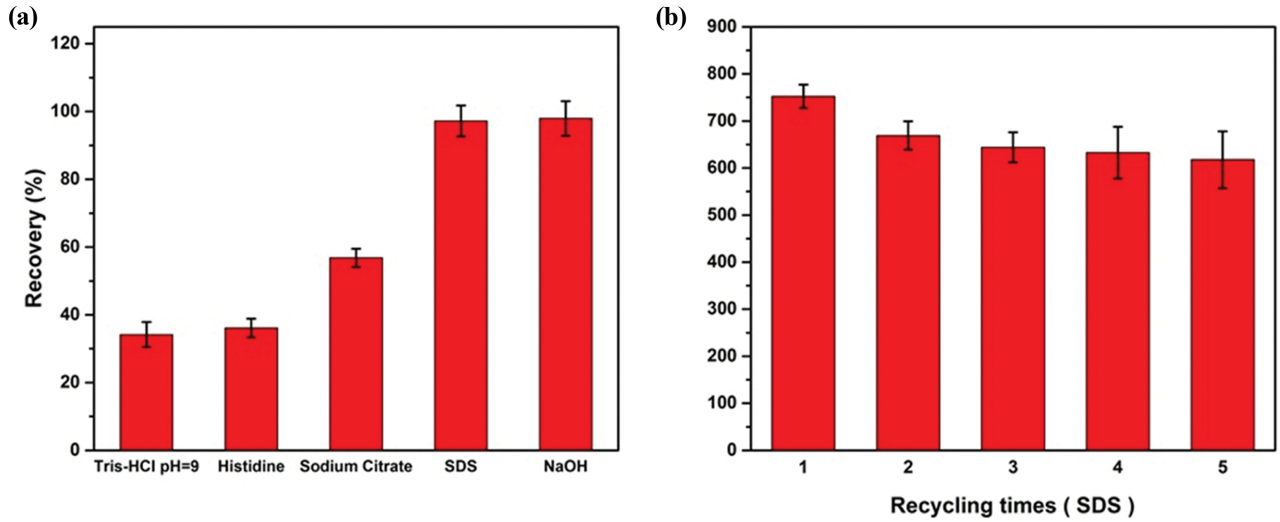


Fig. 8. The elution efficiency of BHb with different eluents (a) and the detailed study of recyclability of $NiFe_2O_4$-PAA-Cu^{2+} microspheres in 0.5%wt SDS (b).

at a mass ratio of 1 : 1 : 4 (Fig. S4(a)). As shown in Fig. S4, after treating with $NiFe_2O_4$-PAA-Cu^{2+} microspheres (Fig. S4(b)), most BHb was adsorbed from the mixed solution while causing small adsorption of BSA and Lyz. Compared with BHb, the adsorption capacities of Lyz and BSA were much minor. And as seen in Fig. S4(c), the captured BHb on $NiFe_2O_4$-PAA-Cu^{2+} microspheres could be released after the treatment of 0.5%wt SDS, while the adsorbed BSA and Lyz were still adsorbed on $NiFe_2O_4$-PAA-Cu^{2+} microspheres.

6. The Reproducibility and Recovery of the Retained BHb on $NiFe_2O_4$-PAA-Cu^{2+} Microspheres

For further study in biology, it is necessary to recover the retained BHb that is adsorbed on the $NiFe_2O_4$-PAA-Cu^{2+} and transfer it into aqueous medium. Therefore, a series of eluting reagents were tested for the ability for recovery of the adsorbed BHb, including 0.1 M Sodium citrate and NaOH, 0.5%wt SDS and histidine, Tris-HCl (pH=9). The result is illustrated in Fig. 8(a). When 0.5%wt SDS and 0.1 M NaOH as eluting reagents got a great elute efficiency, respectively, their elute efficiency could reach 98% and 99%. The recovery of Tris-HCl buffer at higher pH was the lowest (34.15%). The reproducibility of used-resultant in other continuous adsorption/desorption cycle of bovine hemoglobin was considered as an important advantage for follow-up application. The result is shown in Fig. 8(b). With 0.5% SDS solution as the eluting reagent, after five adsorption/desorption cycles, the adsorption efficiency of BHb decreased one by one slightly, still maintaining above 75% adsorption efficiency. On the other hand, as illustrated in Fig. S5, with 0.1 M NaOH as the eluting reagent, the adsorption efficiency was decreased by about 35% in the first adsorption/desorption cycle, and remained at 65% adsorption ability in the third adsorption/desorption cycle. Thus, although using 0.1 M NaOH as eluting reagent could get a better elute efficiency in the first cycle, using 0.5% SDS solution as eluting reagent could gain a similar elute efficiency and increase the number of reuse time of the resulting microspheres.

7. Real Sample Analysis

For the further application of $NiFe_2O_4$-PAA-Cu^{2+} microspheres, the adsorption ability of protein of $NiFe_2O_4$-PAA-Cu^{2+} microspheres for the practical applicability was studied by the selective adsorption of BHb from bovine plasma diluted solution, which was added with certain amount of pure BHb. First, as mentioned in the above experiment section, solution from BP-1 as a part of real sample for pre-testing of microspheres, after adsorption and collected sections. Fig. S6 shows the UV-Vis result of normal 20-fold dilution of bovine plasma (curve c) and before Sample1 bovine plasma (curve a) and after the microspheres adsorption of BP-1 (curve b). The picture shows the adsorbed amount of BHb was significantly higher than other proteins in bovine plasma. This result illustrates

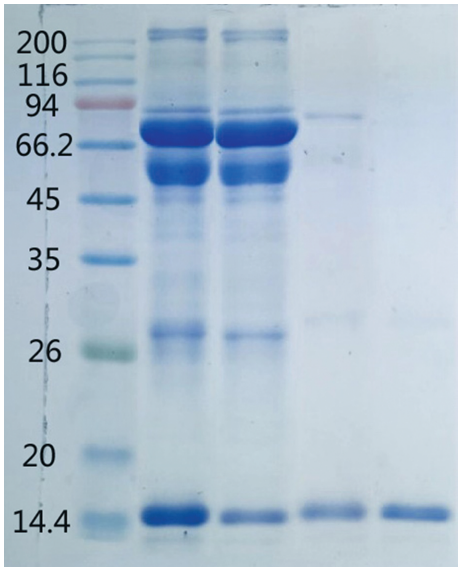


Fig. 9. SDS-PAGE assay result: (Lane 1) Molecular weight standard marker. (Lane 2) Sample from BP-2 without any treatment. (Lane 3) Sample from BP-2 after adsorption by $NiFe_2O_4$-PAA-Cu^{2+} microspheres. (Lane 4): BHb recovered from $NiFe_2O_4$-PAA-Cu^{2+} microspheres. (Lane 5): BHb standard solution of 0.2 mg mL^{-1}.

the resultant microspheres are feasible for pretreatment of real sample analysis.

Furthermore, the practical applicability of $NiFe_2O_4$-PAA-Cu^{2+} for the selective isolation of BHb from BP-2. Bovine plasma sample was processed as mentioned in the experimental section and the supernatant before and after processing by $NiFe_2O_4$-PAA-Cu^{2+} microspheres were collected and 0.2 mg mL^{-1} of BHb was analyzed by SDS-PAGE assay. As illustrated in Fig. 9, we could observe that there were few clear protein bands seen in the diluted bovine plasma with 0.2 mg mL^{-1} of BHb (lane 2), and the protein bands were not significantly changed after treating by microspheres in the supernatant (lane 3); it means there were many other proteins in the bovine plasma. However, in the supernatant after the elution section, we could observe there was only one clear single protein band in the bottom that could be obviously observed (lane 4), and this band was almost the same as the standard BHb band (lane 5). Thus, this result indicates that the resultant microspheres could be applied in the pretreatment of real proteomic sample analysis.

CONCLUSION

This work successfully designed and facilely synthesized a novel magnetic material $NiFe_2O_4$-PAA-Cu^{2+} for selective enrichment and separation of BHb in bovine plasma. This method is advantageous for both facile two-step preparation and low toxicity; the whole synthetic processes are facile and convenient. The Cu^{2+} in synthetic processes was mainly used to chelate with the carboxyl group and strongly bind with the histidine residues of BHb. More importantly, the resultant microspheres showed a high adsorption capacity, fast adsorption kinetics and favorable reproducibility and recovery of the retained BHb abilities. Furthermore, the result demonstrates the resultant microspheres can selectively isolate BHb from prepared bovine serum. This indicates that the resultant microspheres are promising sorbents that can pretreat for the biological sample before proteomic analysis.

ACKNOWLEDGEMENTS

This work was supported by the Natural Science Foundation of China (21575076 and 21621003), the National Key Research and Development Program of China (2016YFA0203101), and the Beijing Municipality Science and Technology Program (D161100002116001).

SUPPORTING INFORMATION

Additional information as noted in the text. This information is available via the Internet at http://www.springer.com/chemistry/journal/11814.

REFERENCES

1. Q. Z. Zhai and X. X. Zhang, *Asian J. Chem.*, **20**, 5060 (2008).
2. B. H. Wang and Q. Shao, *New J. Chem.*, **41**, 5651 (2017).
3. D. J. Graves, *Trends Biotechnol.*, **17**, 127 (1999).
4. Y. Q. Wang and H. M. Zhang, *Int. J. Biol. Macromol.*, **41**, 243 (2007).
5. Y. J. Liu and Y. Z. Wang, *Anal. Chim. Acta*, **936**, 168 (2016).
6. D. Y. Li and Y. Z. Wang, *J. Mater. Chem. B*, **2**, 5659 (2014).
7. K. K. R. Tetala and K. Skrzypek, *Sep. Purif. Technol.*, **115**, 20 (2013).
8. J. D. Wang and S. Y. Tan, *Talanta*, **190**, 210 (2018).
9. C. Din and X. D. Ma, *J. Chromatogr. A*, **1424**, 18 (2015).
10. B. S. Liu and X. N. Yang, *Luminescence*, **29**, 211 (2014).
11. Z. Y. Guo and Y. Zhang, *ACS Appl. Mater. Interfaces*, **8**, 29734 (2016).
12. G. E. Wuenschell, E. Naranjo and F. H. Arnold, *Bioprocess Eng.*, **5**, 199 (1990).
13. Y. Zhang and L. G. Xing, *ACS Appl. Mater. Interfaces*, **7**, 5116 (2015).
14. Q. Zhai and X. Zhang, *Asian J. Chem.*, **20**, 5060 (2008).
15. P. Q. Mu and D. R. Feng, *J. Biochem.*, **150**, 491 (2011).
16. J. J. Wang and R. Zhang, *Talanta*, **176**, 308 (2018).
17. K. F. Du and X. H. Liu, *ACS Sustainable Chem. Eng.*, **6**, 11578 (2018).
18. Ç. Kip and R. B. Tosunb, *Talanta*, **200**, 100 (2019).
19. Z. Y. Guo and Y. Zhang, *ACS Appl. Mater. Interfaces*, **8**, 29734 (2016).
20. Y. Zhang and L. G. Xing, *ACS Appl. Mater. Interfaces*, **7**, 5116 (2015).
21. T. Y. Guo and Y. Q. Xia, *Biomaterials*, **25**, 5905 (2004).
22. X. P. Jia and M. L. Xu, *Analyst*, **138**, 651 (2013).
23. X. W. Kan and Q. Zhao, *J. Phys. Chem. B*, **114**, 3999 (2010).
24. X. D. Yang and M. Zhang, *Appl. Surf. Sci.*, **439**, 128 (2018).
25. M. Zhang and X. W. He, *Nanotechnology*, **22**, 065705 (2011).
26. M. Zhang and X. W. He, *J. Mater. Chem.*, **20**, 10696 (2010).
27. H. Zhang and W. W. Wang, *New J. Chem.*, **42**, 3990 (2018).
28. J. N. Zheng and Z. Lin, *J. Mater. Chem. B.*, **2**, 6207 (2014).
29. Y. W. Zhang and M. Zhang, *J. Alloys Compd.*, **695**, 3256 (2017).
30. J. N. Zheng and Z. Lin, *J. Mater. Chem. B.*, **3**, 2185 (2015).
31. B. Gómez and S. Rubio, *Anal. Chem.*, **81**, 9012 (2009).
32. H. Deng, X. Li and Q. Peng, *Angew. Chem.*, **117**, 2842 (2005).
33. Y. Deng and C. Deng, *Adv. Mater.*, **21**, 1377 (2009).
34. M. S. Niasari and F. Davar, *Polyhedron*, **28**, 1455 (2009).
35. Y. Z. Hua and C. F. Zhaoa, *Chem. Eng. J.*, **349**, 347 (2018).
36. S. Z. Mirahmadi-Zare and A. Allafchian, *Protein Expression and Purification*, **121**, 52 (2016).
37. J. H. Li and M. J. Chen, *Colloids Surf. B: Biointerfaces*, **146**, 468 (2016).
38. W. Wan and Q. L. Liang, *Analyst*, **141**, 4568 (2016).
39. A. H. Lu and E. L. Salabas, *Angew. Chem. Int. Ed.*, **46**, 1222 (2007).
40. M. Faraji and Y. Yamini, *Chem. Soc.*, **7**, 1 (2010).
41. K. Salimi and D. D. Usta, *RSC Adv.*, **7**, 8718 (2017).
42. M. Zhao and C. H. Deng, *Chem. Commun.*, **50**, 6228 (2014).
43. X. Yao and X. D. Ma, *RSC Adv.*, **7**, 29330 (2017).
44. M. Zhang and Y. T. Wang, *Appl. Surf. Sci.*, **375**, 154 (2016).
45. H. Block and B. Maertens, *Methods Enzymol.*, **463**, 440 (2009).
46. S. Maensiri and C. Masingboon, *Scripta Mater.*, **56**, 797 (2007).
47. P. Sivakumar and R. Ramesh, *Mater. Res. Bullet.*, **46**, 2204 (2011).
48. Y. L. Cheng and Y. Zhao, *J. Colloid Interface Sci.*, **344**, 321 (2010).
49. U. Kurtana and H. Güngüneş, *Ceram. Int.*, **42**, 7987 (2016).
50. Q. Yue and J. L. Li, *J. Am. Chem. Soc.*, **137**, 13282 (2015).
51. F. Rouquerol and J. Rouquerol, *Adsorption by powders and porous solids: principles, methodology and applications*, 2nd Ed., Elsevier, Amsterdam, 11 (2014).
52. Y. Zhang and Z. Y. Guo, *Carbon*, **122**, 194 (2017).
53. L. Satyanarayana and K. M. Reddy, *Mater. Chem. Phys.*, **82**, 21 (2003).
54. J. Liu and Y. Z. Bin, *J. Phys. Chem. C*, **116**, 134 (2012).
55. G. Q. Jian and Y. X. Liu, *Nanoscale*, **4**, 6336 (2012).

56. R. X. Gao and X. H. Cui, *Talanta*, **150**, 46 (2016).
57. Y. J. Liu and Y. Z. Wang, *Anal. Chim. Acta*, **936**, 168 (2016).
58. M. Zhang and D. Cheng, *Asian J.*, **5**, 1332 (2010).
59. R. X. Gao and X. R. Mu, *J. Mater. Chem. B.*, **2**, 1733 (2014).
60. J. D. Wang and H. Y. Guan, *ACS Biomater. Sci. Eng.*, **5**, 2740 (2019).
61. E. B. Altıntas and D. Türkmen, *Colloids Surf. B: Biointerfaces*, **85**, 235 (2011).
62. Y. Zhang and L. G. Xing, *ACS Appl. Mater. Interfaces*, **7**, 5116 (2015).
63. L. Shi and Y. H. Tang, *J. Sep. Sci.*, **39**, 2876 (2016).

Supporting Information

A facile method to synthesize magnetic nanoparticles chelated with Copper(II) for selective adsorption of bovine hemoglobin

Huiyuan Guan, Jundong Wang, Siyuan Tan, Qiang Han, Qionglin Liang†, and Mingyu Ding†

MOE Key Laboratory of Bioorganic Phosphorus Chemistry and Chemical Biology, Ministry of Education, Department of Chemistry, Tsinghua University, Beijing 100084, China

(*Received 5 December 2019 • accepted 5 March 2020*)

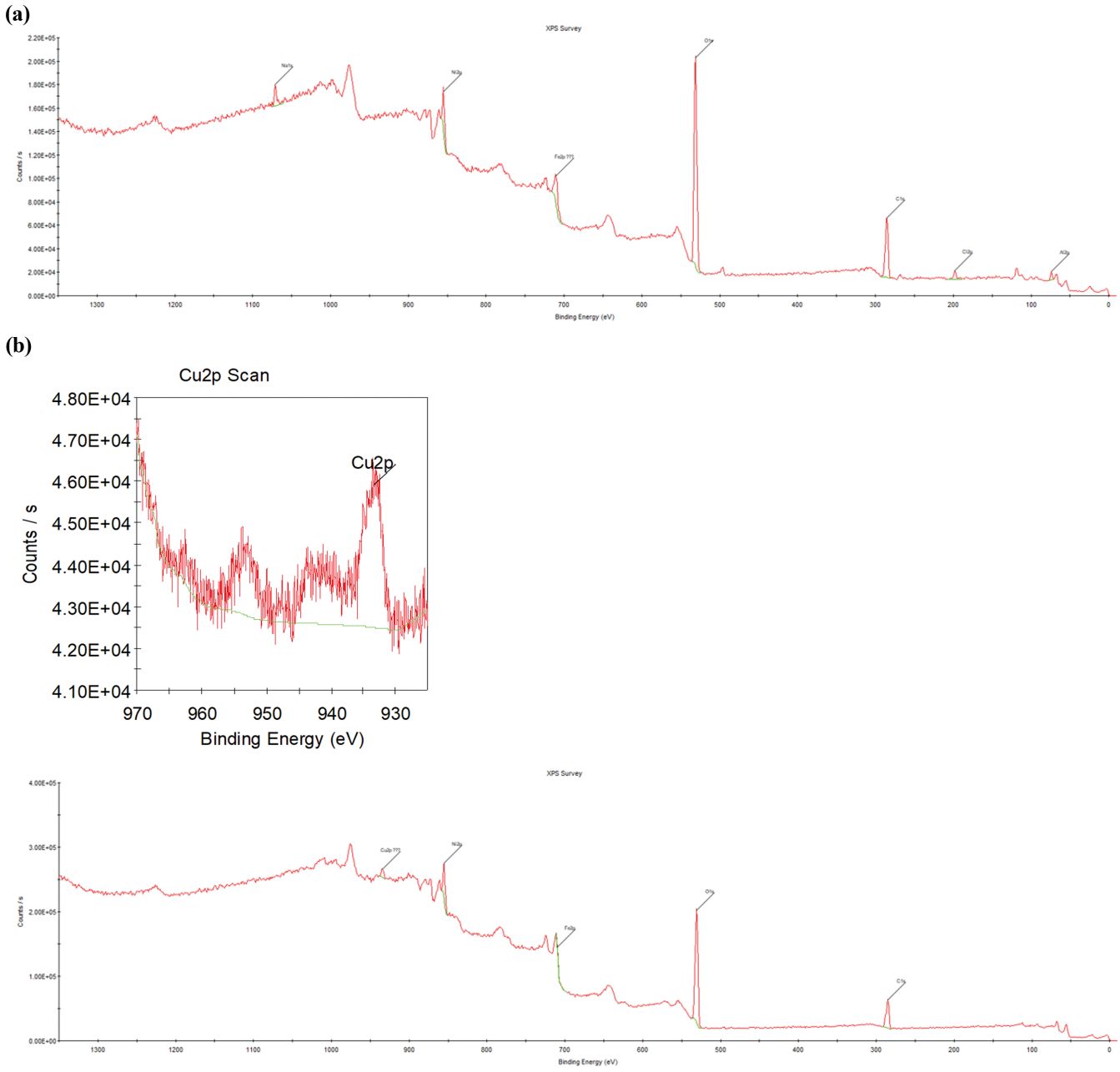


Fig. S1. XPS spectra of $NiFe_2O_4$-PAA microspheres (a). XPS spectra of $NiFe_2O_4$-PAA-Cu^{2+} microspheres (b).

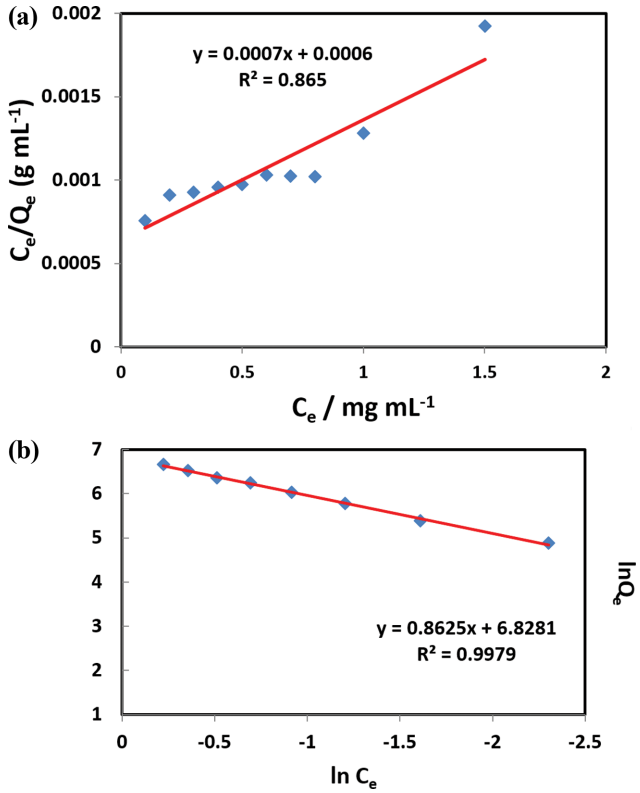


Fig. S2. The Langmuir (a) and Freundlich (b) adsorption isotherm fit of BHb.

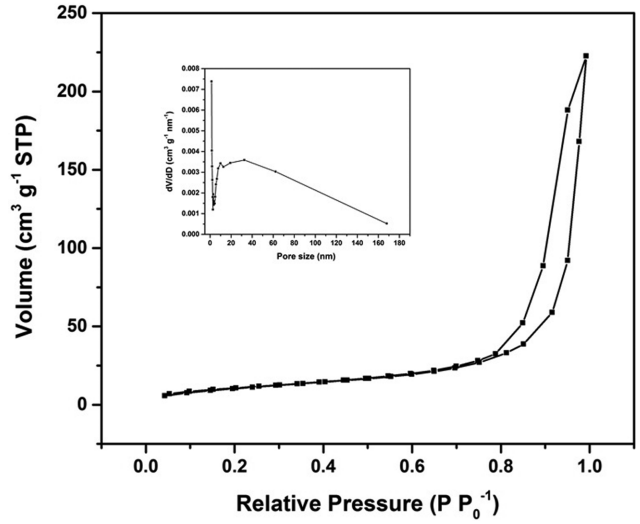


Fig. S3. N_2 adsorption/desorption isotherms and pore size distribution curve of $NiFe_2O_4$-PAA microspheres.

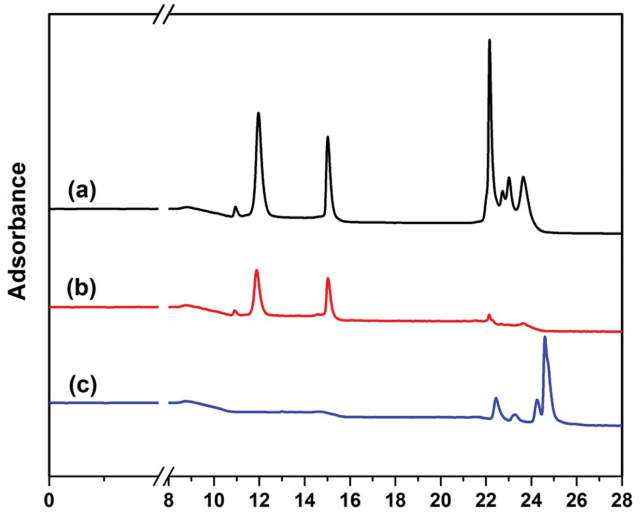


Fig. S4. HPLC results of protein mixture of 0.2 mg mL^{-1} Lyz, 0.2 mg mL^{-1} BSA and 0.8 mg mL^{-1} BHb (a), the supernatant after treating with $NiFe_2O_4$-PAA-Cu^{2+} microspheres (b), and the eluate from $NiFe_2O_4$-PAA-Cu^{2+} microspheres-protein conjugates (c).

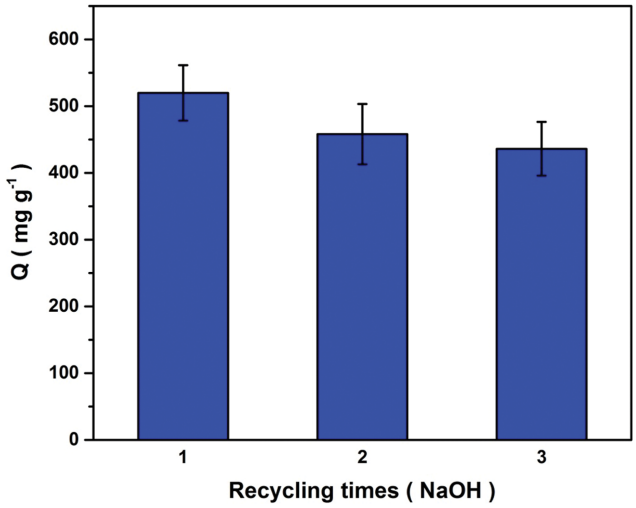


Fig. S5. The recyclability of the $NiFe_2O_4$-PAA-Cu^{2+} microspheres in 0.1 M NaOH.

1. Evaluation of Adsorption Capacity

The adsorption capacity (Q_e, mg g^{-1}) was calculated according to the following formula:

$$Q=(C_0-C_e)\cdot V/m$$

Where C_0 (mg/mL) is the initial concentration of BHb, and C_e (mg/g) is the final concentration of BHb after adsorption, V (mL) is the volume of BHb solution. m is the mass of $NiFe_2O_4$-PAA-Cu^{2+} microspheres.

The adsorption isotherms were calculated by Langmuir model and Freundlich model.

$$C_e/Q=K_l/Q_{max}+C_e/Q_{max}$$
$$LnQ=lnK_f+lnC_e/n$$

Where C_e is the equilibrium concentration (mg/mL) of BHb, Q (mg/g) is the equilibrium adsorption capacity, Q_{max} (mg/g) is the saturated capacity. K_l and n are the Langmuir constant and Freundlich constant, respectively.

In the adsorption isotherms experiments, 1 mg of microspheres was incubated with 1 mL of protein solution for 3 h with different

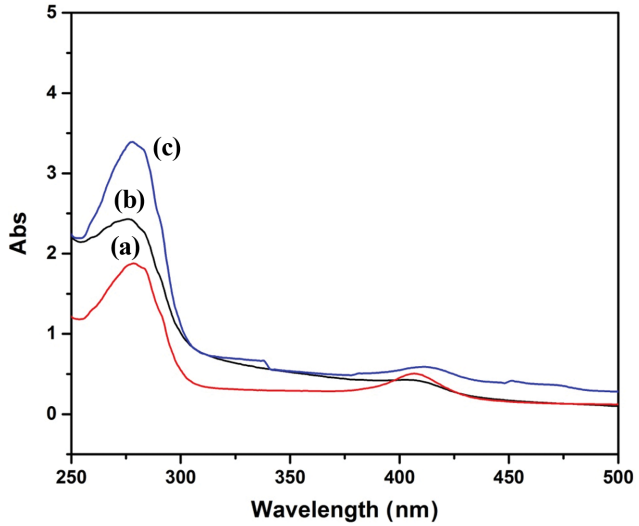


Fig. S6. The UV-Vis spectrum result of bovine plasma (c) and spiked with 0.1 mg/mL BHb in bovine plasma (a) and after the microspheres adsorption of spiked with 0.1 mg/mL BHb in bovine plasma (b).

concentrations ranging from 0.05 to 1.5 mg mL^{-1}.

In the adsorption kinetic binding experiments, 1 mg of microspheres was mixed with 1 mL of protein solution for different times ranging from 1 to 180 min.